Friction Stir Welding and Processing-V
TMS (The Minerals, Metals & Materials Society), 2009

CONTROL OF STRUCTURE IN CONVENTIONAL FRICTION STIR WELDS THROUGH A KINEMATIC THEORY OF METAL FLOW

H.A. Rubisoff[1], J.A. Schneider[1], and A.C. Nunes, Jr.[2]

[1]Mississippi State University;
P.O. Box ME; Mississippi State, MS 39762
[2]NASA Marshall Space Flight Center
MSFC, Huntsville, AL 35812

Keywords: friction stir welding, AA2219, material flow

Abstract

In friction stir welding (FSW), a rotating pin is translated along a weld seam so as to stir the sides of the seam together. Metal is prevented from flowing up the pin, which would result in plowing/cutting instead of welding, by a shoulder on the pin. In conventional FSW, the weld metal rests on an "anvil", which supports the heavy "plunge" load on the tool. In this study, both embedded tungsten wires along and copper plating on the faying surfaces were used to trace the flow of AA2219 weld metal around the C-FSW tool. The effect of tool rotational speed, travel speed, plunge load, and pin thread pitch on the resulting weld metal flow was evaluated. Plan, longitudinal, and transverse section x-ray radiographs were examined to trace the metal flow paths. The results are interpreted in terms of a kinematic theory of metal flow in FSW.

Introduction

FSW is a solid state joining process developed by The Welding Institute [1]. Since the development of FSW, researchers have worked to model weld metal flow in the vicinity of the tool and its relation to the weld structure. Early theories suggested a "chaotic-dynamic mixing" in the material [2]. Later tracer studies, using steel shot [3], aluminum shims [4], copper foil [5], bi-metallic welds [6-7], and tungsten wire [8], revealed defined streamline flow paths of the tracers interpretable in terms of an orderly flow of metal around the pin-tool. However, the effect of process parameters on the resulting metal flow is still not physically understood [9, 10]. This becomes increasingly important in designing robust tooling and process schedules to avoid defects such as wormholes.

The rotating weld tool used in FSW consists of a shoulder which rides along the workpiece surface, and a threaded cylindrical pin, which extends through the material thickness. As this weld tool rotates, the rotation motion causes deformation of the material adjacent to the surface of the shoulder and the intruding pin. This study considers the effects of process parameters and tool design on FSW microstructures and relates the microstructures to flow field components in a kinematic model of FSW metal flow.

Figure 1 illustrates the kinematic model of the FSW flow field [9]. The model decomposes the flow field around the pin into three incompressible flow field components, any combination of which yield an incompressible FSW flow field. These components are a rigid body rotation

around the pin, a uniform translation as the tool transverses the weld seam, and a ring vortex flow field around the tool established by threaded pin features. The flow components combine to create two currents in the flow field: a "straight-through" current of which the flow elements remain within the rotating flow for less than a complete rotation of the tool and a "maelstrom" current of which the elements remain within the rotating flow for multiple rotations [9].

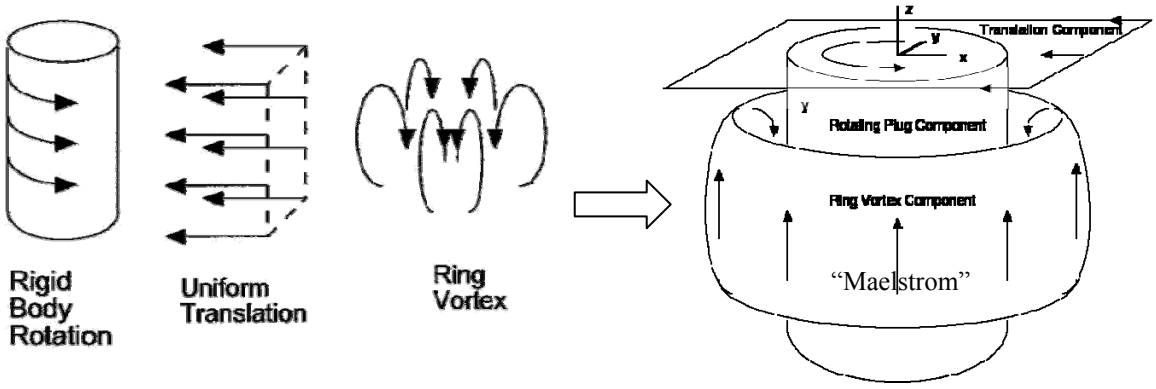

Figure 1. The flow around a FSW pin tool can be decomposed into three components: 1) a rigid body rotating plug component, 2) a translation component, and 3) a ring vortex component. Apparently, complex FSW structural features can be understood in terms of these three components and their interactions. These components can be related to welding parameters and tool design. The components present a conceptual bridge between weld process, which can be controlled, and weld structure (and weld properties).

The rigid body rotation field component comprises metal attached to the tool and rotating with the tool. It is bounded by a surface attached to the tool and a shearing surface, observed to be very thin, with the rotating plug of metal attached to the tool on one side and the body of weld metal moving at a relatively slow weld speed with respect to the tool on the other side. Metal crossing this boundary is subjected to extreme shear rates (typically 10^3 to 10^5 sec^{-1}) comparable to those of metals crossing a similar shear plane in metal cutting operations. As the rotating field moves through the metal, it entrains elements of metal, rotates them, and abandons them in the wake of the weld tool.

The ring vortex field component superposes a radial velocity component and an axial velocity component on the flow field at the shearing surface. A negative radial velocity component retains metal elements longer in the rotating flow and tends to shift their exit into the weld cross section toward the advancing side (AS) of the tool. Some of the flow may be retained for many revolutions flowing axially and exiting only where the radial flow velocity component shifts from inward to outward. This effect has been reported in other studies where markers have traced out metal paths rotating multiple times around the weld tool [11]. The ring vortex flow field outside the shear surface adds distortions of its own to the weld structure.

It is generally possible, as will be demonstrated here, to attribute changes in tracer patterns to changes in the flow field components of the kinematic model, and to relate the flow field component changes to changes in weld parameters and tool geometry. Thus, through the kinematic model it is possible to relate weld parameters and tool geometry to weld structure and to control weld structure.

Experimental Procedure

AA2219-T87 panels 0.25″ thick were used in this study. The weld tool was machined from tool steel with a left hand pitch of 20 threads per inch. Pure copper (98.7%) was thermally sprayed to a thickness of 0.006″ along the faying surface of one panel to mark the seam. Tungsten wires of 0.001″ diameter were also placed longitudinally along the weld seam at depths of 20%, 50%, and 80% of the panel thickness or 0.05″, 0.13″, and 0.20″ respectively from the shoulder surface. One panel was used for each wire depth providing 3 repetitions of processing parameters for each copper plated faying surface.

The weld parameters in this study included rotation speed, travel speed, and force. The weld schedule for each panel is described in Table I. Each panel was welded using a systematic variation of one parameter as illustrated in Figure 2 to yield 3 weld specimens per panel. After the tungsten wire was positioned in a grove at the required depth, run on tabs were tack welded in place to hold the panels together.

Table 1. Weld schedule for conventional and self-reacting friction stir weld panels

a) FSW schedule

Panel	Rotational Speed (rpm)	Travel Speed (ipm)	Downward Force (lbs)	Wire position (in)	speed/rotation (in/rev)
C7	200	4.5	6500, 7000, 8000	0.05	0.023
C8	200	4.5	6500, 7000, 8000	0.13	0.023
C9	200	4.5	6500, 7000, 8000	0.20	0.023
C22	150, 200, 300	4.5	7000	0.05	0.03- 0.015
C23	150, 200, 300	4.5	7000	0.13	0.03-0.015
C24	150, 200, 300	4.5	7000	0.20	0.03-0.015
C37	200	3, 4.5, 6	7000	0.05	0.015- 0.030
C38	200	3, 4.5, 6	7000	0.13	0.015- 0.030
C39	200	3, 4.5, 6	7000	0.20	0.015- 0.030

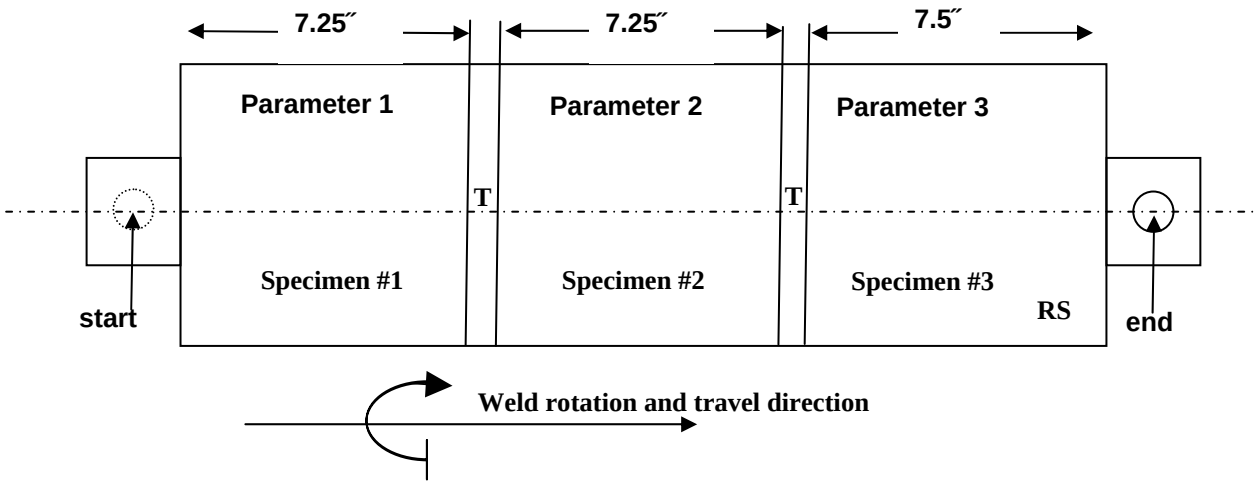

Figure 2. FSW panel layout showing run-on tabs on the 2 ends. A 1″ transition (T) section separates the parameter variations. One panel was used for each embedded wire placement depth.

Once all the panels were welded, x-ray radiographs of the welds were taken in 3 views, Figure 3. Plan x-rays recorded the as-welded panels. To radiograph in the longitudinal direction, the width of the weld panels was trimmed to isolate the weld region. Next, the samples were sectioned to an approximate thickness of 0.25″ and radiographed in the transverse direction. The 0.25″ transverse thickness captured 8-16 revolutions of the weld tool.

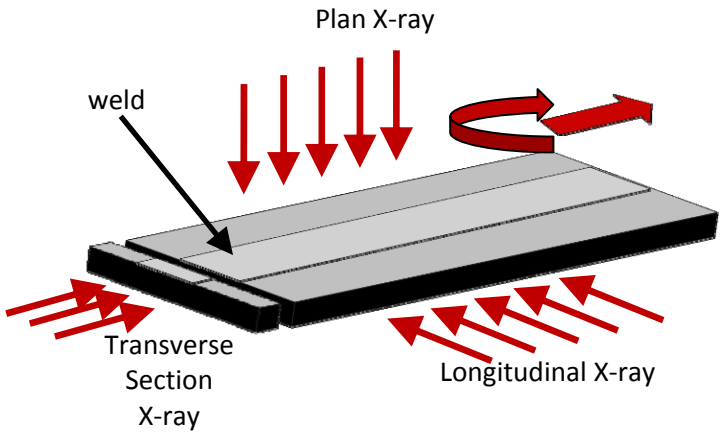

Figure 3. Layout directions of x-ray radiographs were taken of the weld region.

The x-ray radiographs were then examined to locate and highlight the post weld position of the tungsten wire and copper plating to determine what parameters affect material flow and how the process parameters move material through the weld nugget. Corresponding metallographic samples were prepared of the plan and transverse views to compare marker placement with variations observed in macro images.

Results and Discussion

Metal flow around the weld tool can be considered as a bundle of stream lines, Figure 4a. As the metal is wiped around with the weld tool, a shear zone exists in the workpiece separating the region of fine metal grains from the relatively coarse grains of the parent material microstructure. Figure 4b is a plan view of a friction stir weld metallographically polished to remove the deformation induced by the shoulder. The fine grained region surrounding the cavity where the weld tool was removed is circular and displaced toward the RS so that a thicker region is noted on the RS than on the AS.

Weld markers introduced from the weld stream into the rotating flow are whisked around and deposited in the wake of the weld. Ignoring the effect of the ring vortex flow component, i.e., lateral and axial shifts, a wire marker exits along the same line as it enters the rotating flow. Figure 5 show plan views of tungsten wire markers introduced close to and distant from the shoulder. Two features are noteworthy. The wire is fragmented in the rotating flow. The fragments exhibit appreciable lateral scatter close to the shoulder.

Fragmentation occurs when the shear forces of the metal in the rotating flow on the segment of wire introduced into the rotating flow produce a sufficient load at the anchor point of the wire to tear the wire apart. When this happens, the wire segment is swept away in the rotational flow around the pin and out into the weld structure in the wake of the tool. Copper marker deposits on weld seam surfaces are torn apart into fragments in a similar fashion. Hence, in subsequent

radiographs, streamlines are marked by discontinuous fragments of copper. Bundles of streamlines averaged in radiographs may look like a continuous line or, where broadly distributed, like a field of separate fragments. Metallographic images, which exhibit a very thin surface plane only, do not show continuous traces, but only discontinuous fragments from which drawing conclusions regarding streamlines may not be feasible.

Scatter occurs due to oscillation of the diameter of the shear surface. This varies the conditions of exit from the rotating field in a complex way and produces a complex series of lateral displacements in the tracer [12]. The shear surface is anchored to the tool shoulder at the edge of a no-slip surface for which the friction force is greater than the metal flow stress. Periodically, metal is emitted from under the shoulder. This periodic emission process forms the peaks and valleys of the "tool marks" on the weld surface and the band structures that appear as "onion rings" in weld transverse sections. As metal escapes from under the shoulder edge, local normal pressure may drop making slip against the shoulder edge easier than shear within the metal. The anchor point of the shear surface follows the onset of slip on the shoulder and oscillates. The oscillation and the scatter induced by it are thus greatest at the shoulder and diminish away from the shoulder. The scatter effect tends to produce broader distributions of marker fragments toward a tool shoulder.

For present purposes, marker fragmentation and scatter are artifacts that need to be recognized to avoid confusion but that do not significantly obscure the interpretation of the data in terms of the basic kinematic model

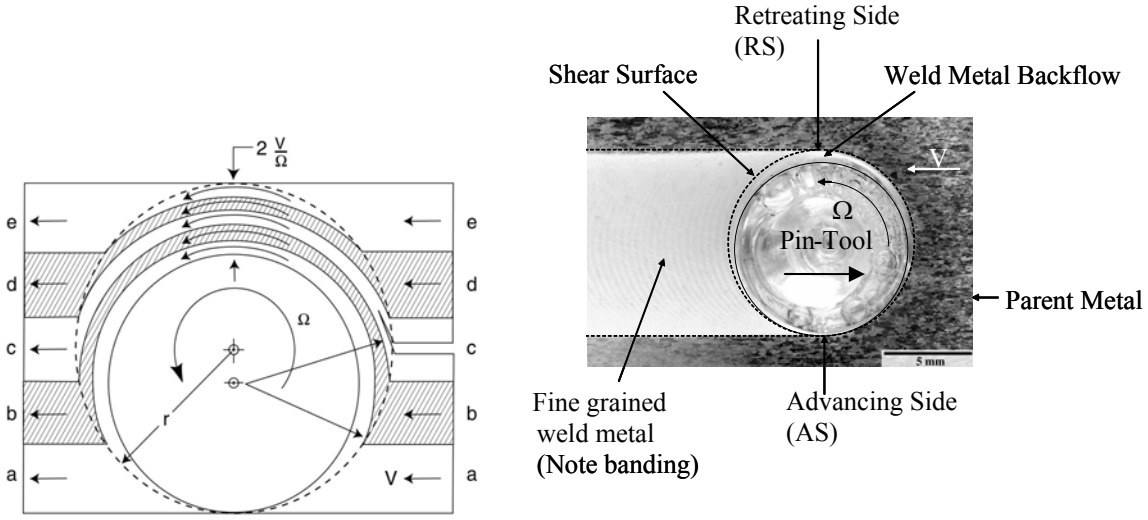

(a) **(b)**

Figure 4. (a) Expected stream line flow of weld metal due to rotational motion of the weld tool. (b) Metallographic mount of the plan view of a friction stir weld termination showing differences in the refined metal region on the AS versus RS of the weld pin.

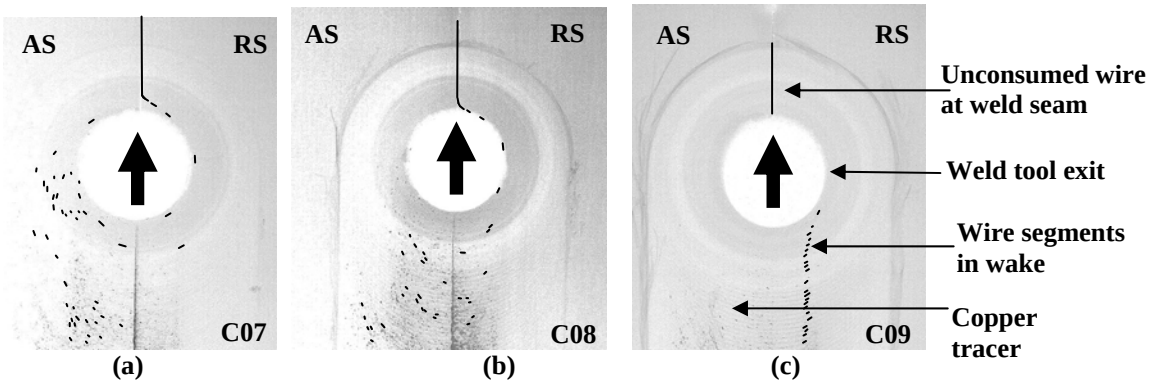

Figure 5. Plan inverted x-ray of friction stir welds processed at 200 RPM, 4.5 ipm, and 8000 lbs plunge force. Tungsten wire segments have been digitally enhanced to document post weld position of (a) 0.05″, (b) 0.13″ and (b) 0.20″ below shoulder surface.

Inverted x-ray radiographs of the transverse surface of a 0.25″ thick friction stir weld are shown in Figure 6 for the range of travel and plunge force investigated in this study. The dark region corresponds to the deposit of copper originally located on the faying surface of the weld seam. Within the parameter range investigated for travel and plunge load, little variation in the resulting copper tracer placement is observed. If the copper on the faying surface were simply whisked around the pin tool, a vertical band of copper at the position of the initial weld seam location would be seen. Evidence of the trace from the former shoulder and pin surfaces can be observed on the AS of the transverse section. The copper bands in Figure 7 show distortions from a purely vertical band with the heaviest concentration of copper located on the RS. In all the weld sections of Figure 7, the expected trace loop is observed extending from the shoulder AS to the pin RS and back around to the original seam location. But this "primary loop" is somewhat obscured by a secondary distortion. This slight distortion is observed as a slight dip about mid thickness of the weld panel bringing the copper trace back to the position of the former seam location.

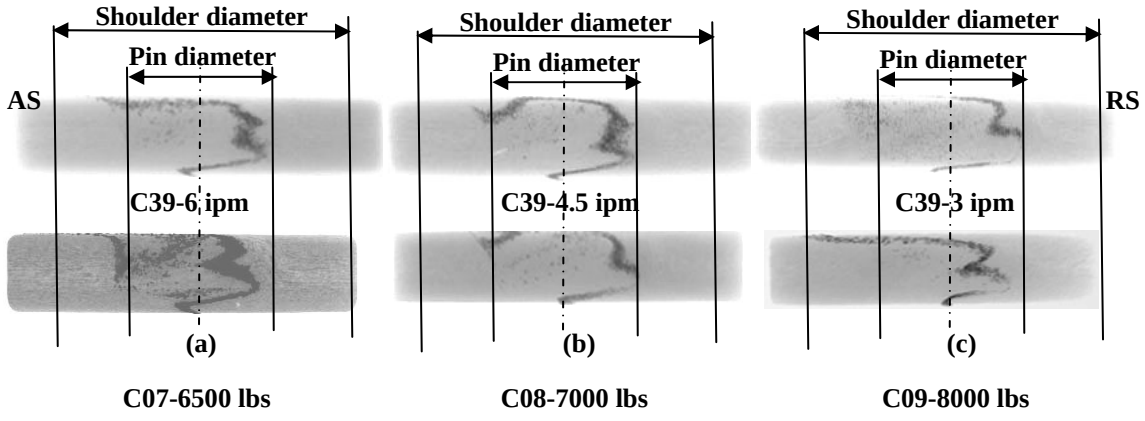

Figure 6. Minimal variation observed in an inverted x-ray of post weld copper tracer due to variations in travel (a) and plunge force (b). Weld tool rotation was held constant at 200 RPM. As the weld travel was varied (a), the plunge force was held constant at 7000 lbs and as the plunge load was varied (b), the travel was held constant at 4.5 ipm. The dashed line indicates the centerline of the former weld seam location.

In comparison, Figure 7 shows changes in the shape of the copper tracer as the RPM is varied. Figure 7 also includes corresponding transverse section metallographs of the friction stir weld

mounted, polished, and etched to reveal the microstructure. Banding (onion rings) and other etch-sensitive structures that do not show up on the radiographs are visible in the metallograph. Deformation of the band by the flow field around the pin can also be seen. A rise in the band in the outer portion of the ring vortex component of the flow field is conspicuous on the RS of the pin.

The copper is observed as dark particles in the weld zone of the metallographs shown in Figure 7. Although the copper particles fall along the trace of the weld seam identified in the radiograph, their density is insufficient to mark this trace very clearly. Hence the complimentary radiographs of 0.25″ thick transverse slices of the weld, which average the copper density, provide a more continuous marking of the former seam trace.

The radiographs and metallographs reveal distortions due to the flow field around the pin. At the edge of the ring vortex component, the flow is axially upward toward the tool shoulder. An axial displacement of the band toward the shoulder increasing with the RPM is conspicuous on the RS (right) of the pin, caused by a through thickness component.

Using the flow paths predicted by the Nunes model, illustrated in Figure 1, the ring vortex circulation can be envisioned to flow inward under the tool shoulder, down the threads on the pin, outward toward the bottom of the pin, and upward on the outside to complete the circulation with conserved weld metal volume. Inward flow delays the exit of weld metal from the rotating plug flow and shifts the trace metal toward the AS of the tool, Figure 8. Outward flow hastens the exit of weld metal from the rotating plug and shifts the trace metal toward the RS of the tool. Hence, because of the interaction of the rotating plug and ring vortex flow components, one expects to see the trace of the weld seam mark out a line from the shoulder AS to the pin RS. Since the outflow does not extend all the way to the bottom of the weld, the displacement effect on the seam trace vanishes at the anvil, and the seam trace reverts back to its original position.

Using the kinematic model, the seam trace at 150 RPM (Figure 7a), the left extending advancing arm of the seam trace, starts to show a swirl characteristic. The “notch” in the “primary loop” at 150 RPM can be attributed to a ring vortex secondary distortion. As the RPM is increased from 150 to 200 RPM (Figure 7b), this notch becomes more pronounced as the arm develops an axial characteristic. As the temperatures within the weld zone increase, the amount of softened material that can be drawn into the ring vortex increases. This increases until the notch is no longer observed at 300 RPM (Figure 7c) as the ring vortex flow appears to dominate the microstructure. It is also at the 300 RPM condition that a defect is observed to open up as a classic ‘wormhole’, Figure 7c.

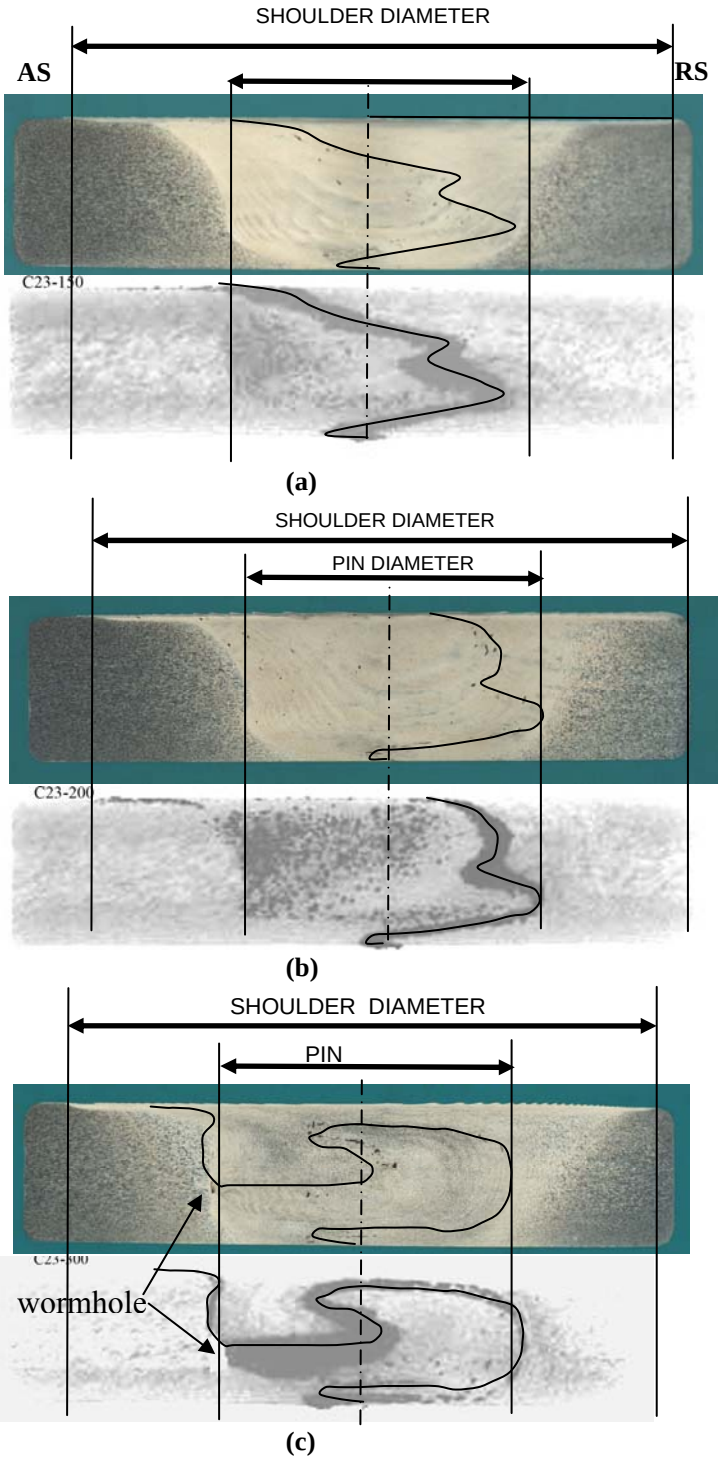

Figure 7. Transverse friction stir weld radiographs of the trace of the weld seam marked by a deposit of Cu at varying rotational speeds. The travel speed was maintained at 4.5 ipm and the plunge force at 7000 lbs with the rotation varied from: (a) 150 RPM, (b) 200 RPM, to (c) 300 RPM. All welds show the basic advancing-(shoulder-side-to-retreating-(pin)-side-and-back-to-center loop due to the interaction of the rotating plug and ring vortex flow field components. At higher RPM, greater distortions of the basic loop appear as the ring vortex flow extends out from the shear surface.

To explain the variation observed in the traced flow, Figure 8 illustrates the metal at the former seam being influenced by a ring vortex flow. This causes metal to remain in the rotating plug longer as the weld tool transverses along the initial seam. Figure 8a illustrates a mild influence of the ring vortex flow on the metal in the rotational plug, where the effect is to move the material downward, but not necessarily remaining within the rotating plug for multiple weld tool rotations. As the region of plasticized metal increases in hotter welds to where the ring vortex flow exerts a stronger influence on the rotating plug (Figure 8b), regions of the metal would stay within the rotational plug flow longer, possibly for several rotations.

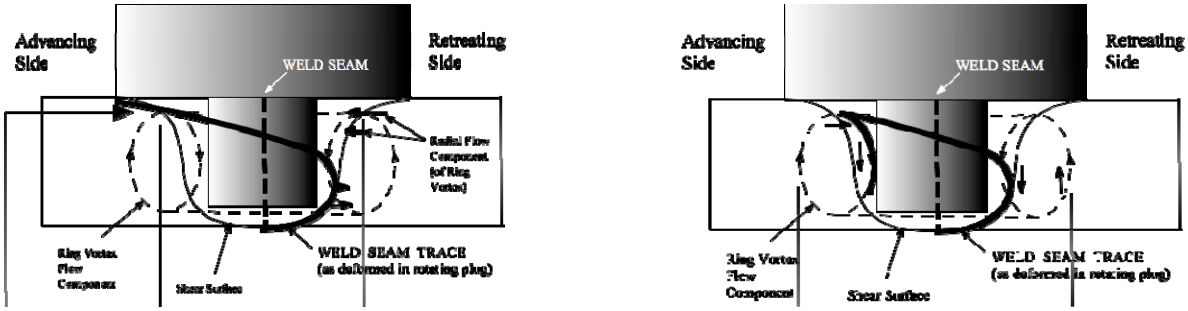

(a) (b)

Figure 8. Projected trace of copper tracer coated on the faying surface prior to the FSW. (a) In a colder weld, the ring vortex flow offers minimal distortion to the radial deformation. (b) As the weld becomes hotter and the zone of plasticized material increases, the ring vortex would be expected to draw more material into its flow path.

Once the rotational flow of the rotating plug has moved past the trace elements embedded in the tool wake, ring vortex circulations outside the rotating plug continue to distort the seam trace. If the outer edge of a ring vortex flow passes over a metal volume, it imparts a rotary swirl to that volume in the transverse plane. If the center of the ring vortex flow passes over a metal element, it imparts an up-and-down axial motion to it in the transverse plane. There are temperature gradients in FSW [13], and plastic flow around the tool tends to be restricted to hotter regions where the weld metal flow stress is lower. Hence, in hotter (higher RPM) welds the ring vortex flow field is more broadly extended as can be observed on the RS of the metallograph in Figure 7c.

Summary

For FSW, the rotational speed affects how the shoulder interacts with the work piece. This interaction means that increasing the rotational speed results in a decreased impact on the weld metal path induced by the shoulder. As the weld heats, the shoulder and the bottom of the pin begin to have less effect on the material movement. This can also be considered to be the transition between sticking and slipping at these interfaces.

This understanding of the influence of process parameters on material flow during FSW also offers insight into defect formation. In a hotter weld, obtained by higher RPMs, the vortex dominates the metal flow causing a disruption in the continuity of flow provided by the translational component.

Acknowledgements

The assistance of Carolyn Russell, Joseph Querin, Rhonda Lash, John Ratliff and Ronnie Renfroe is gratefully acknowledged. Funding from the Mississippi Space Grant and Marshall Space Grant Consortiums contributed to this study.

References

[1] Thomas, W.M., Nicholas, E.D., Needham, J.C., Murch, M.G., Temple-Smith, P., and Dawes, CJ. *Friction-stir butt welding*. GB Patent No. 9125978.8, International Patent No. PCT/GB92/02203 (1991).

[2] Li, Y., Murr, L.E., McClure, J.C., "Flow visualization and residual microstructures associated with the friction-stir welding of 2024 aluminum to 6061 aluminum, *MSEA*, Vol. A271, p. 213-223, 1999.

[3] Colligan, K., "Material flow behavior during friction stir welding of aluminum," *Welding Res. Suppl*., p. 229s-237s, July 1999.

[4] Seidel, T.U., Reynolds, A.P., "Visualization of the material flow in AA2195 friction-stir welds using a marker insert technique," *Met. & Mat. Trans*., Vol. 32A, p. 2879-2884, 2001.

[5] Guerra, M., Schmidt, C., McClure, J.C., Murr, L.E., Nunes, A.C., Jr., "Flow patterns during friction stir welding," *Mat'ls Characterization*, Vol. 49, p. 95-101, 2003.

[6] Contreras, F., Trillo, E.A., Murr, L.E., "Friction-stir welding of a beryllium-=aluminum powder metallurgy alloy," *J. Mat. Sci*., Vol. 37, p. 89-99, 2002.

[7] Ouyang, J.H., Kovacevic, R., "Material flow and microstructure in the friction stir butt welds of the same and dissimilar aluminum alloys," *J. Mat. Eng. & Perf*., Vol. 11, p. 51-63, 2002.

[8] Schneider, J.A., Nunes, A.C., Jr., "Quantifying the material processing conditions for an optimized FSW process", *7th Int'l Conf. Trends Welding Research*, 2005.

[9] Schneider, J.A., Nunes, Jr., A.C., "Characterization of plastic flow and resulting micro textures in a friction stir weld," *Met. Trans. B*, V. 35, p. 777-783, 2004.

[10] Arbegast, W.J., "Modeling friction stir joining as a metal working process," *Hot Deformation of Aluminum Alloys*, ed. Z. Jin., TMS, 2003.

[11] London, B., Mahoney, M., Bingel, W., Calabrese, M., Bossi, R.H., Waldron, D., *FSW&P* II, eds. K.V. Jata, M.W. Mahoney, R.S. Mishra, S.L. Semiatin, T. Lienert, p. 3-12, 2003.

[12] Schneider, J.A., Beshears, R., Nunes, Jr., A.C., "Interfacial sticking and slipping in the friction stir welding process", *Mat'l Sci. & Engr. A,* Vol. 435-436, p. 297-304, 2006.

[13] Mahoney, M.W., Rhodes, C.G., Flintoff, J.G., Spurling, R.A., Bingel, W.H., "Properties of friction-stir-welded 7075-T651 aluminum," *Metall. Mater. Trans*., Vol. 29A, p. 1955-1964, 1998.

CONTROL OF STRUCTURE IN CONVENTIONAL FRICTION STIR WELDS THROUGH A KINEMATIC THEORY OF METAL FLOW

H.A. Rubisoff and J.A. Schneider

Mississippi State University
Mississippi State, MS 39762

A.C. Nunes, Jr.

NASA Marshall Space Flight Center
MSFC, Huntsville, AL 35812

Objective

Interpret the material flow path during the friction stir weld process:

- Model validation
- Control of weld microstructure
- Optimize pin tool geometry and weld parameters

Friction Stir Welding

- Developed at The Welding Institute in 1991
- First used on aluminum alloys
- Solid-state process

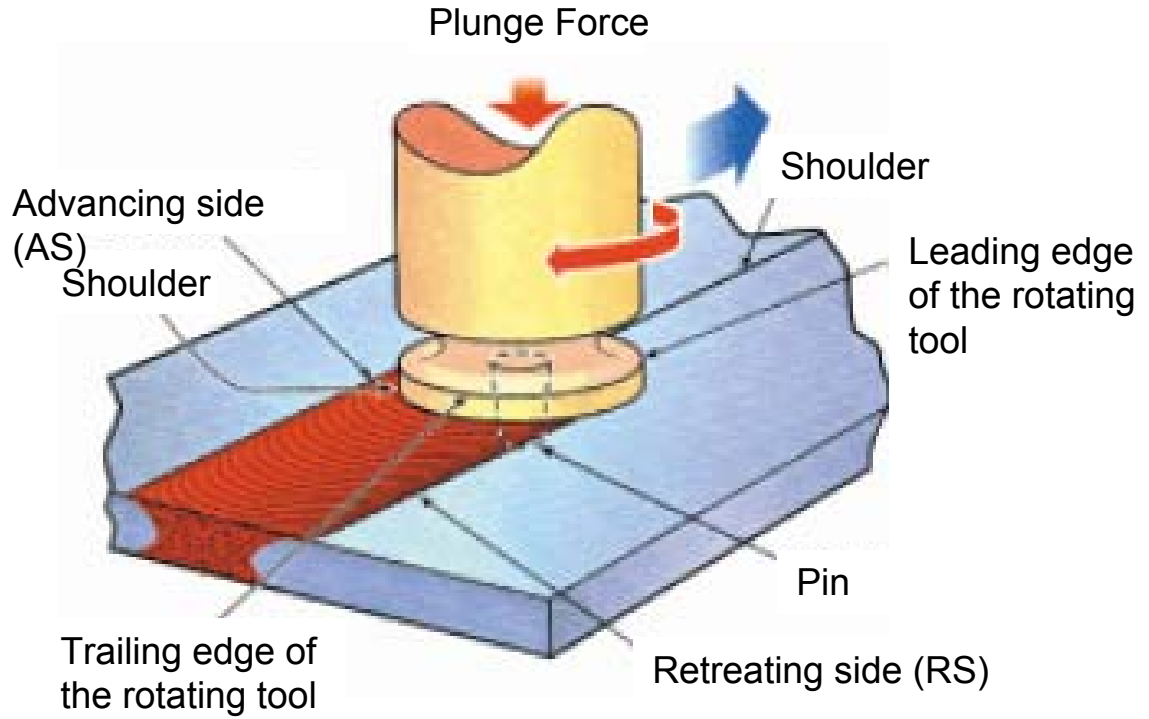

Defined streamline flow paths of the tracers interpretable in terms of an orderly flow of metal around the pin-tool

- Tracer studies:
  - steel shot [Colligan, Welding Res. Supp., 1999]
  - aluminum shims [Seidel, et al., Met. & Mat. Trans. A, 2001]
  - copper foil [Guerra, et al., Mat'ls Charact., 2003]
  - bi-metallic welds [Contreras, et al, Mat. Sci., 2002, Ouyang, et al., Mat. Eng. & Perf., 2002]
  - tungsten wire [Schneider, et al., 7th Int'l Trends in Welding, 2005]
- However, the effect of process parameters on the resulting metal flow is not physically understood [Schneider, et al., Met. Trans. B, 2004, Arbegast, TMS, 2003]

Stream line theory can be used to describe the flow of metal around the weld tool

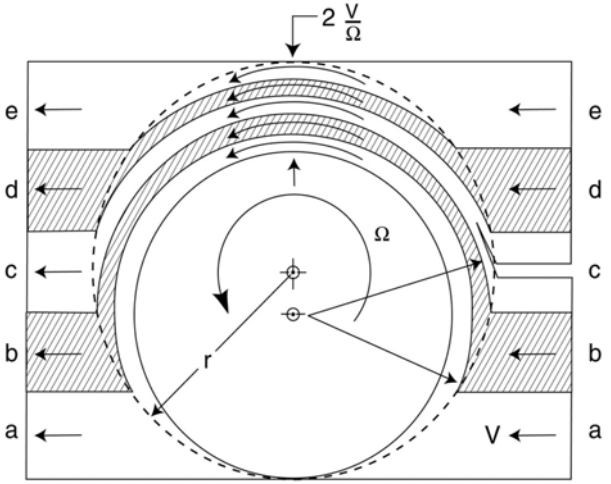

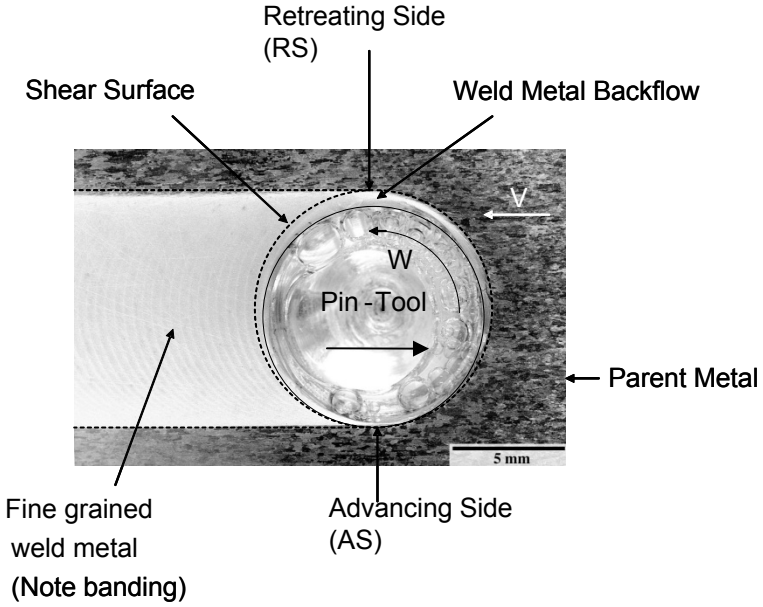

A thicker region of material is noted on the retreating side of the weld

[Nunes, Internal NASA Memo, 2001]

Fragmentation of a tungsten wire tracer documents more scatter with wire closer to the shoulder

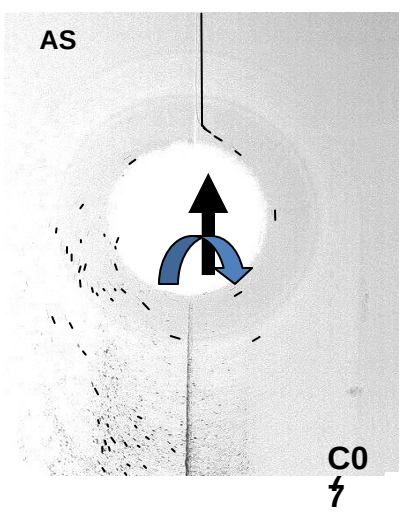

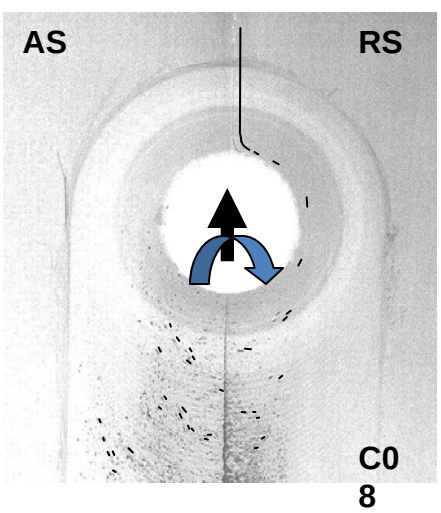

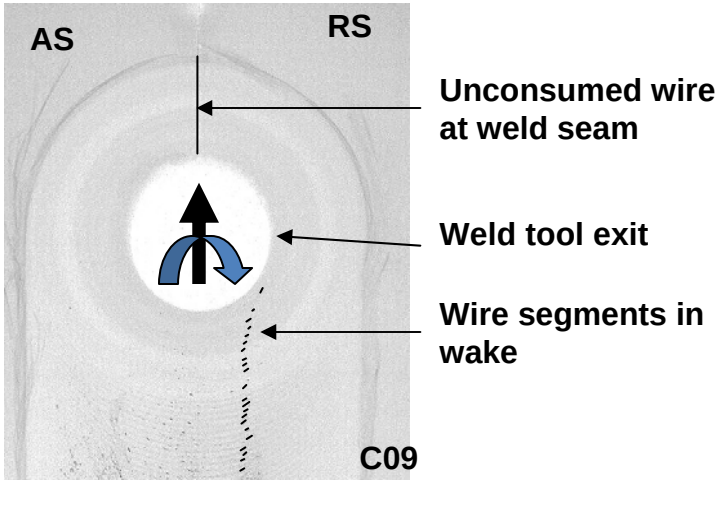

Tungsten wire depth	0.05” (20% matl thk)	0.13” (50% matl thk)	0.20” (80% matl thk)

Plan inverted x-ray radiograph of FSWs processed at 200 RPM, 4.5 ipm, and 8000 lbs

A kinematic model of the FSW flow field defines 3 incompressible flow fields which combine to form 2 flow streams

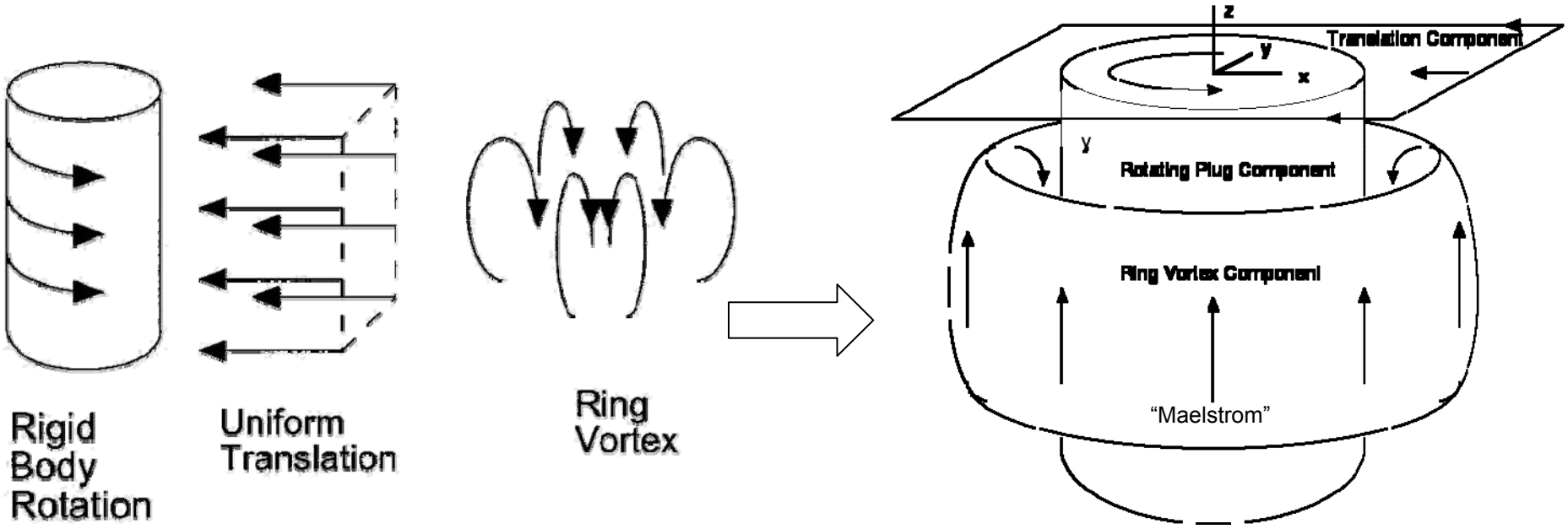

[Schneider & Nunes, Met. Trans. B, 2004]

Experimental Procedure

Objective: trace faying surfaces

<u>Wire placement:</u>
0.05”, 0.13”, and 0.12” below shoulder surface

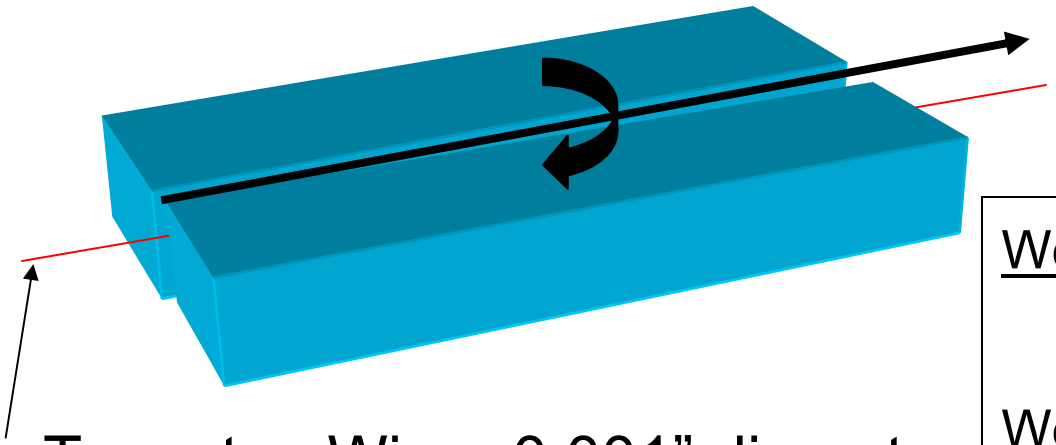

- Tungsten Wire: 0.001” diameter
- Cu plating: 0.006˝
- Al 2219-T87 plates: 0.25” thick

[Colligan, Welding Journal, 1999]
[Seidel & Reynolds, Met. & Mat. Trans. A, 2001.]

<u>Weld parameters:</u>
Load Control
Varying load, RPM, & travel

<u>Weld Tool:</u>
tool steel
LH thd: 0.5-20 UNJF
1.2” dia scrolled shoulder

<u>Weld Panels:</u>
3 repetitions per parameter set

Weld Parameter Matrix

Panel	Rotational Speed (rpm)	Travel Speed (ipm)	Downward Force (lbs)	Wire position (in)	speed/rotation (in/rev)
C7	200	4.5	6500, 7000, 8000	0.05	0.023
C8	200	4.5	6500, 7000, 8000	0.13	0.023
C9	200	4.5	6500, 7000, 8000	0.20	0.023
C22	150, 200, 300	4.5	7000	0.05	0.03- 0.015
C23	150, 200, 300	4.5	7000	0.13	0.03-0.015
C24	150, 200, 300	4.5	7000	0.20	0.03-0.015
C37	200	3, 4.5, 6	7000	0.05	0.015- 0.030
C38	200	3, 4.5, 6	7000	0.13	0.015- 0.030
C39	200	3, 4.5, 6	7000	0.20	0.015- 0.030

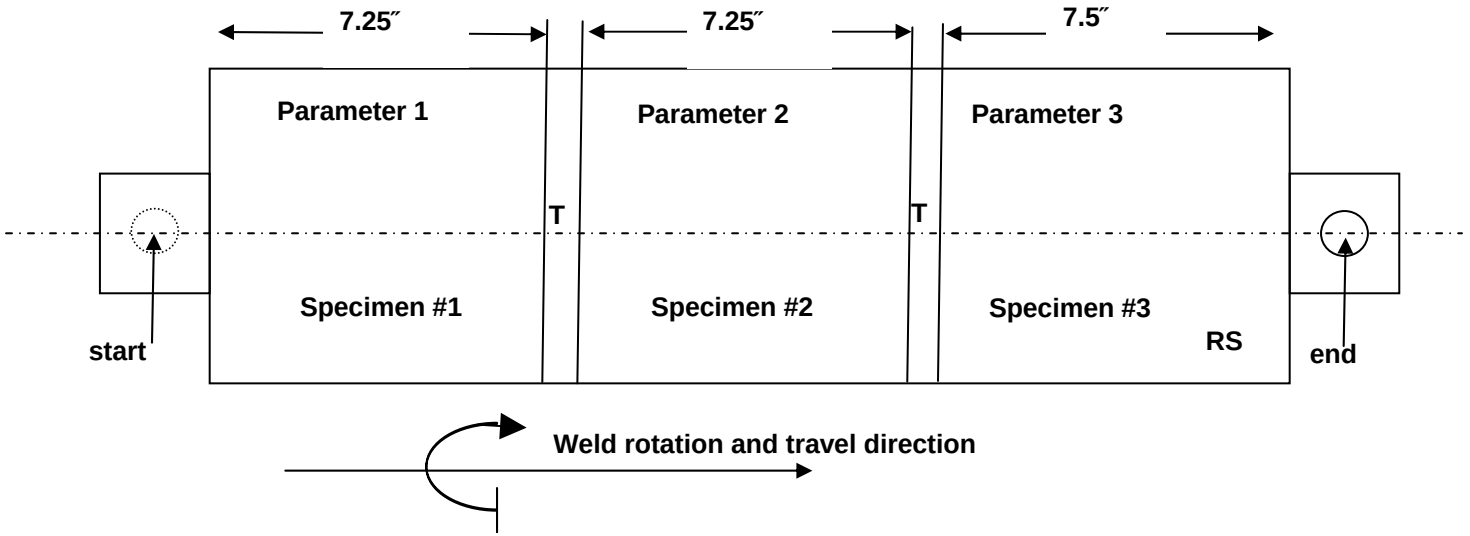

Projected faying surface movement

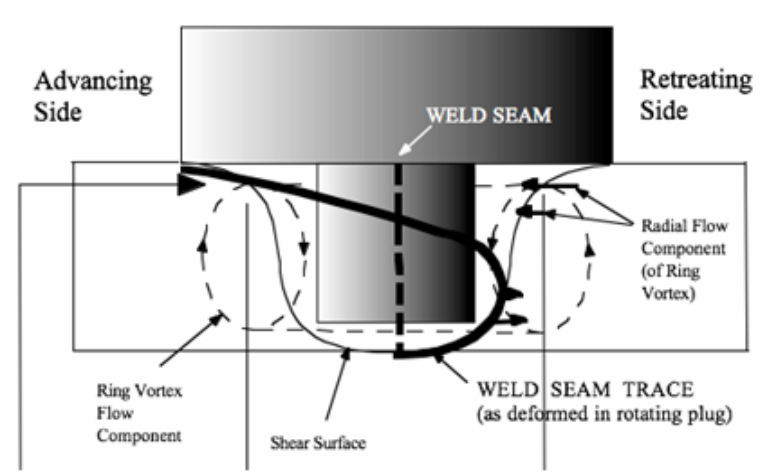

Cooler weld
(lower RPM)

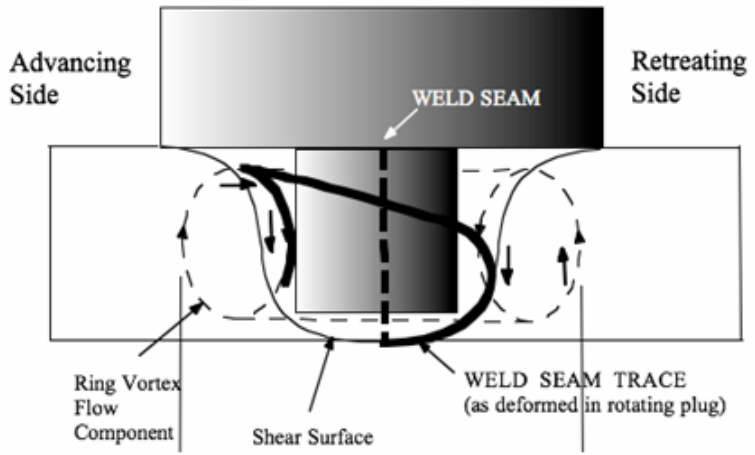

Hotter weld
(higher RPM)

As the vortex flow acts upon the rotating plug of metal, the post weld placement of the seam would be expected to be distorted.

Former weld seam can be observed in x-ray radiographs of transverse views.

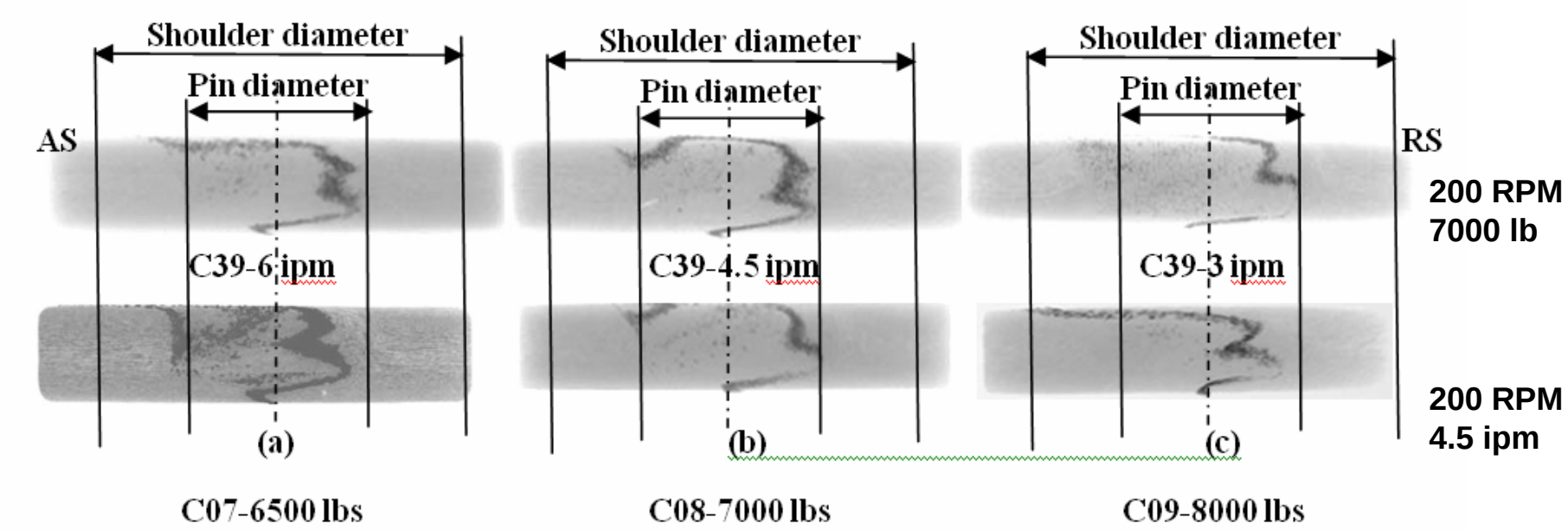

No significant differences noted with variations in travel speed and plunge force

Significant changes to weld seam trace observed with RPM variation

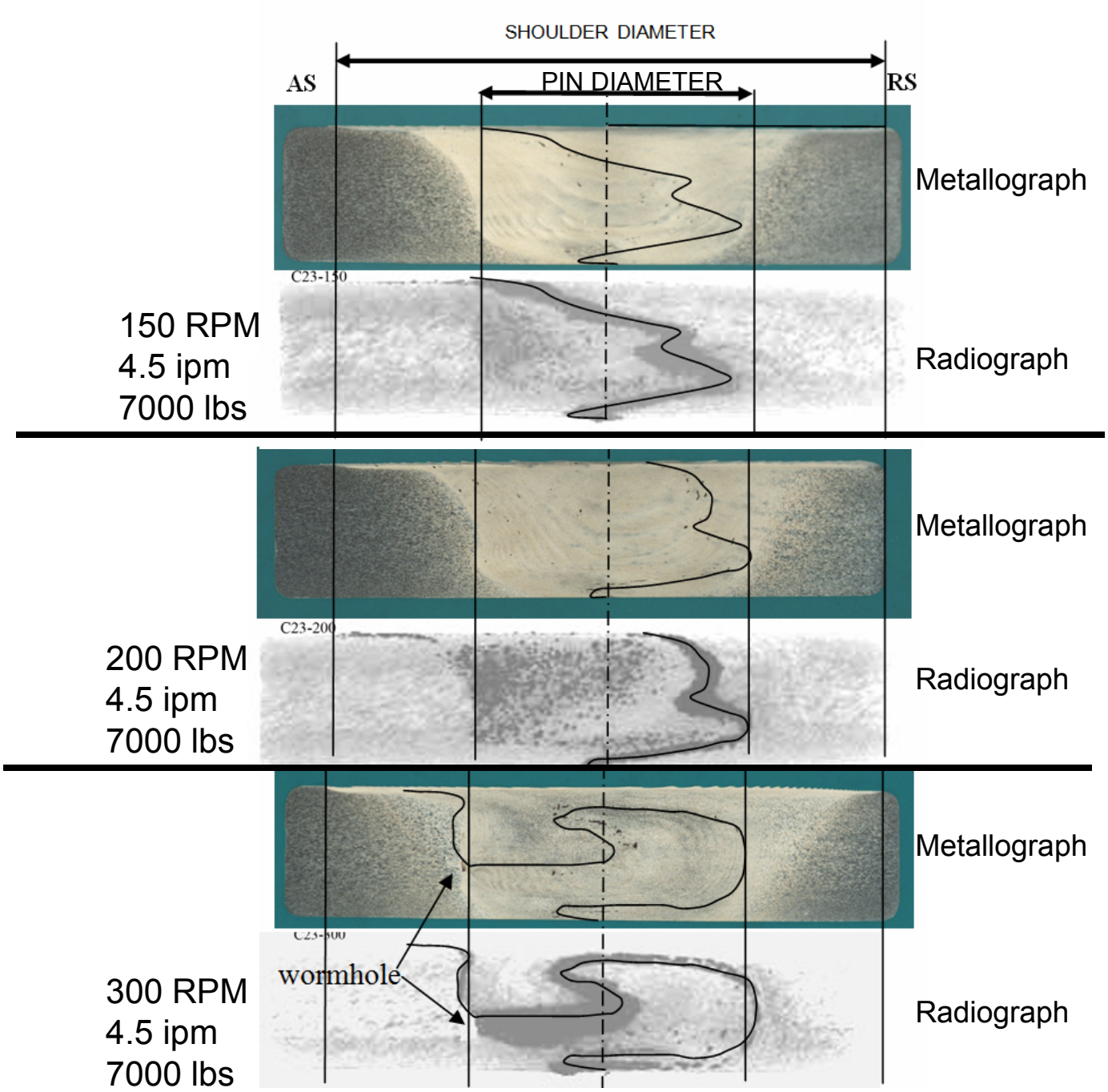

Summary

- Rotational speed affects how the shoulder interacts with the work piece.
  - Increased rotational speed = decreased impact on the weld metal path induced by the shoulder
- As the weld heats, the shoulder and the bottom of the pin begin to have less effect on the material movement.
  - transition between shoulder sticking and slipping
- Understanding of the influence of process parameters on material flow during FSW offers insight into defect formation.
  - In a hotter weld, obtained by higher RPMs, the vortex dominates the metal flow causing a disruption in the continuity of flow provided by the translational component.

Acknowledgements

Funding was provided in part by:

Mississippi Space Grant (MSSGC) and

Marshall Space Grant Consortiums MSGC.

The assistance of Carolyn Russell, Rhonda Lash, John Ratliff, and Ronnie Renfroe at the NASA-MSFC is gratefully acknowledged.